JOURNAL OF EXPERIMENTAL ZOOLOGY 311A:240–257 (2009)

A Journal of Integrative Biology

Kinematics of Level Terrestrial and Underwater Walking in the California Newt, *Taricha torosa*

MIRIAM A. ASHLEY-ROSS*, REBECCA LUNDIN, AND KRISTY L. JOHNSON
Department of Biology, Wake Forest University, Winston-Salem, North Carolina

ABSTRACT Salamanders are acknowledged to be the closest postural model of early tetrapods and are capable of walking both in a terrestrial environment and while submerged under water. Nonetheless, locomotion in this group is poorly understood, as is underwater pedestrian locomotion in general. We, therefore, quantified the movements of the body axis and limbs of the California newt, *Taricha torosa*, during steady-speed walking in two environments, both of which presented a level surface: a treadmill and a trackway that was submerged in an aquarium. For treadmill walking at a relative speed of 0.63 snout–vent lengths (SVL)/sec, newts used a diagonal couplets lateral sequence walk with a duty factor of 77%. In contrast, submerged speeds were nearly twice as fast, with a mean of 1.19 SVL/sec. The submerged gait pattern was closer to a trot, with a duty factor of only 41%, including periods of suspension. Environment appears to play a critical role in determining gait differences, with reduction of drag being one of the most important determinants in increasing duration of the swing phase. Quantitative analysis of limb kinematics showed that underwater strides were more variable than terrestrial ones, but overall were strikingly similar between the two environments, with joint movement reversals occurring at similar points in the step cycle. It is suggested that the fundamental walking pattern appears to function well under multiple conditions, with only minor changes in motor control necessary. *J. Exp. Zool. 311A:240–257, 2009.*

How to cite this article: Ashley-Ross MA, Lundin R, Johnson KL. 2009. Kinematics of level terrestrial and underwater walking in the California newt, *Taricha torosa*. J. Exp. Zool. 311A:240–257.

The ability to move is a hallmark of the animal kingdom. Human interest in animal locomotion has been present since ancient times (Gray, '68), and researchers have examined forms of movement as diverse as bat flight (e.g., Swartz et al., '92; Lindhe-Norberg et al., 2000), galloping in horses (e.g., Deuel and Park, '93; Biewener, '98), bipedal running in lizards (e.g., Snyder, '49; Irschick and Jayne, '99) and swimming in fish (e.g., Dowis et al., 2003; Liao, 2004) and secondarily aquatic mammals (e.g., Fish, '98). Although the extreme performance of these animals excites our admiration and interest, a fruitful line of inquiry lies in examination of less extreme, more flexible types of locomotion, such as those that must function in multiple environments (e.g., Frolich and Biewener, '92; Gillis, '97; Fish and Baudinette, '99; Fish, 2000; Ellerby et al., 2001; Gillis and Blob, 2001; Johansson and Lindhe-Norberg, 2001; Ashley-Ross and Bechtel, 2004; Nauwelaerts et al., 2007). Salamanders are an excellent model group in which to examine nonspecialized locomotion; not only are they capable of walking (on land and in water; Ashley-Ross and Bechtel, 2004) and swimming (Frolich and Biewener, '92; Gillis, '97), but they are generally considered to be the closest postural model for early tetrapods among extant taxa (Edwards, '77, '89) and salamander morphology has been fundamentally static for at least 150 million years (Gao and Shubin, 2001).

Grant sponsor: National Science Foundation; Grant number: IBN 0316331.
*Correspondence to: Miriam A. Ashley-Ross, Department of Biology, Box 7325, Wake Forest University, Winston-Salem, NC 27109. E-mail: rossma@wfu.edu
Received 18 September 2008; Revised 26 November 2008; Accepted 22 December 2008
Published online 5 March 2009 in Wiley InterScience (www.interscience.wiley.com). DOI: 10.1002/jez.522

Salamanders employ a sprawling posture, in which the limbs extend laterally out from the body and the feet are placed to the sides, as opposed to an erect posture, in which the weight of the body is balanced over the limbs (Rewcastle, '81; Reilly and Elias, '98). Although the erect posture is thought to be more efficient and advanced (Rewcastle, '81; Hildebrand, '85), it has proven a difficult model for workers in the field of biologically inspired robotics, owing to difficulties with balance. Instead, such researchers have turned to the salamander as their model of choice in trying to build a robot capable of coordinated, autonomous locomotion (Ijspeert, 2000, 2001; Taylor and Massey, 2001; Breithaupt et al., 2002; Ijspeert et al., 2007). Thus, from both an evolutionary and a biomechanic/biomimetic standpoint, limbed locomotion in salamanders is important to understand.

Previous quantitative studies of salamander walking are sparse; several have focused primarily on axial movements (Daan and Belterman, '68; Edwards, '77; Frolich and Biewener, '92), whereas those that have concentrated on the limbs have examined relatively few species (*Ambystoma tigrinum*, Peters and Goslow, '83; *Necturus maculatus*, Wheatley et al., '92; *Dicamptodon tenebrosus*, Ashley-Ross, '94a,b, '95; *Pleurodeles waltl*, Delvolve et al., '97; *Taricha torosa,* Ashley-Ross and Bechtel, 2004). Of the preceding, only the studies of *Dicamptodon* and *Taricha* have presented quantitative limb kinematics.

In this study, we quantify the kinematics of level walking performed in terrestrial and aquatic environments; terrestrial locomotion was captured on a treadmill, whereas aquatic walking was performed on a trackway submerged in shallow water. *Taricha* is a particularly appropriate species for locomotion studies, because individual newts migrate long distances annually during the breeding season (Petranka, '98). We hypothesize that because of the buoyant support of water, submerged walking will be characterized by changes consistent with a reduced-gravity model: lower duty factors and more variable kinematics, as has been shown for underwater pedestrian rock crabs (Martinez et al., '98). We compare the data from California newts to that of other sprawling tetrapods, highlighting similar features, but suggest that additional research on motor patterns controlling walking in different environments needs to be done in order to reach a fuller understanding of the biomechanics and evolution of limbed locomotion.

METHODS

Animals

Five metamorphosed California newts *(T. torosa)* were purchased from local pet suppliers. The individuals were housed in a common 40 L terrarium with ad libidum access to water. They were fed a diet of waxworms and small crickets 2–3 times a week. Snout–vent lengths (SVL) of the animals ranged from 5.95 to 7.04 cm at the time of the experiments. Walking trials were performed at room temperature (~25°C). All experimental protocols were approved by the Wake Forest University Institutional Animal Care and Use Committee.

Video recording

Terrestrial walking

Newts were videotaped walking on a variable-speed, motor-driven treadmill. For scale, lines of 10 cm apart were marked on the treadmill surface, and a 1 cm grid was drawn on the back wall of the treadmill. To assist identification of anatomical landmarks, a series of light-colored dots were painted (Testor's flat model paint) over the shoulder, elbow, wrist, hip, knee and ankle joints, and along the midline starting with the pectoral girdle and ending at the pelvic girdle. Seven points were painted along the vertebral column between the two limb girdles.

Video images from the dorsal view were captured by a JVC GR-DVL9800 digital camcorder (JVC America, Wayne, NJ), and lateral images were captured by a Redlake MotionScope 1000S (Redlake Imaging Corp., Morgan Hill, CA) high-speed video system. Both cameras captured images at a rate of 60 fields per second. Video records from the two cameras were synchronized by a discrete event visible in both the dorsal and lateral views.

Submerged walking

Newts walked along a trackway submerged in a partially filled aquarium. The trackway was surfaced with nonslip bathtub tread strips to provide traction for the animals. A series of dots of 1 cm apart was marked on the trackway surface for scale. A vertical 1 cm grid next to the trackway allowed calibration of lateral images. Artificial markers were not painted on the newts in the submerged trials, as the dots would simply float away in the water. However, repeated digitizing trials of the same sequence demonstrated that we

could digitize anatomical landmarks with accuracy (variation in x, y coordinate positions over three digitizing passes of the same sequence was $<2\%$).

Video sequences were captured with two JVC GR-DVL9800 digital camcorders placed to afford dorsal and lateral views. Recording rate for both cameras was 60 fields per second. Video records from the two cameras were synchronized by a discrete event visible in both views.

Video analysis

Only sequences in which the newt showed continuous, steady-speed motion were selected for analysis. Strides where the animal started or stopped moving were not used. A minimum of five strides were analyzed from each animal; strides selected for analysis came from more than one trial. Video recordings were captured into a Macintosh computer using either Adobe Premiere 6.5 (Adobe Systems, Inc., San Jose, CA) or Final Cut Express 2 (Apple Computer, Inc., Cupertino, CA). Video files were exported as sequences of still images. DeBabelizer Pro 5 (Equilibrium Technologies, San Rafael, CA) was used to de-interlace the two fields of each frame and convert the images to JPEG format. The custom video analysis program Didge (written by Alistair Cullum of Creighton University, and available for download at http://biology.creighton.edu/faculty/cullum/Didge/) was used to determine the (x,y) coordinates for anatomical landmarks (see below). Sequences of images from the dorsal and lateral views were digitized independently. From both views, the following points were digitized: the tip of the snout, the vertebral column midway between the shoulder joints, the vertebral column midway between the hip joints, and on the limbs nearest the front wall of the treadmill or aquarium, the shoulder, elbow, wrist, hip, knee, and ankle joints. Additionally, the joints of the limbs on the side of the newt away from the lateral camera were digitized in the dorsal view. To reduce digitizing error, the raw coordinates were smoothed by Gaussian filtering in Igor Pro 4.09 (WaveMetrics, Lake Oswego, OR). The smoothed coordinates were then imported into Microsoft Excel (Microsoft Corp., Redmond, WA), which was used to compute the angle variables defined below. For two-dimensional angles, only the coordinates from the dorsal view were used. For three-dimensional angles, the vertical coordinates from the lateral view were used as the z-coordinates. True three-dimensional angles were computed by Maple 6 (Maplesoft, Waterloo, Ont., Canada). The curves produced by plotting these angle values for each sequence (the ''kinematic profile'') were then used for determination of minimum and maximum values for each kinematic variable (defined below).

Definition of variables

A *stride* was defined as the time (in sec) from left hindfoot contact with the substrate surface to the subsequent contact of the same foot. The following angles were measured in two dimensions: *Pectoral girdle angle* was defined as the angle between the line connecting the shoulder joints (''pectoral girdle line'') and the direction of travel (taken as the line connecting the points on the vertebral column at the pectoral and pelvic girdles). *Pelvic girdle angle* was defined as the angle between the line connecting the hip joints (''pelvic girdle line'') and the direction of travel. *Trunk angle* was defined as the angle between the lines connecting the point over the vertebral column midway along the trunk to the points centered over the limb girdles. *Pectoral girdle–humerus angle* was measured between the pectoral girdle line and the line connecting the shoulder joint and the elbow. *Pelvic girdle–femur angle* was measured between the pelvic girdle line and the line connecting the hip joint and the knee. These angles were 180° when the humerus/femur was in line with their respective girdle line, less than 180° when the humerus/femur was inclined forward of that line (protracted), and greater than 180° when inclined back of that line (retracted). The following angles were measured in three dimensions: *Humerus–forearm angle* was measured between the line segments connecting the shoulder to elbow joint (''humerus line'') and the elbow to wrist joint (''forearm line''). *Femur–crus angle* was measured between the line segments connecting the hip to knee joint (''femur line'') and the knee to ankle joint (''crus line''). Finally, *humerus–substrate angle, forearm–substrate angle, femur–substrate angle*, and *crus–substrate angle* were defined as the angles between the appropriate limb segment lines and the surface of the treadmill or submerged trackway, as appropriate.

Several timing variables were also measured: the durations of contact of each of the feet with the substrate, and the relative timing between the beginning of the stride and the minima and maxima of the angular variables described above. Timing variables were standardized by dividing the step cycle duration; thus, each is expressed as

a percentage of stride. The portion of the stride during which the foot is in contact with the substrate is the *stance phase* (the corresponding proportion of the stride is termed the *duty factor*), whereas the portion of the stride in which the foot is elevated and being moved into position for the start of the next stride is termed the *swing phase*.

Because each stride may have differing relative proportions of stance and swing phase, the angular variables for the terrestrial strides were further normalized by converting them into the corresponding values for a standardized stride consisting of 75% stance and 25% swing, following the formula described in Ashley-Ross ('95). This procedure was not followed for the submerged strides, as the duty factor differed substantially from 75% (see ''Results''). Hildebrand -style footfall diagrams (Hildebrand, '66, '76) were also generated by plotting duty factors as a percentage of the step cycle.

Statistical analysis

Kinematics for level treadmill and submerged walking were analyzed for statistically significant differences in SPSS 15.0 for Windows (SPSS Inc., Chicago, IL) using MANOVA that considered environment and individual as the main effects. Environment was treated as a fixed effect, whereas individual was treated as a random effect. Subsequent ANOVAs identified individual variables that differed according to environment. In all tests, environment was tested over the environment × individual interaction term; other effects were tested over the residual. Differences were considered significant at $\alpha = 0.05$; owing to large numbers of comparisons being made, the sequential Bonferroni method of Rice ('89) was used to establish the corrected significance level. Additionally, data were explored in multivariate space using the Ggobi 2.0 data visualization program (Swayne et al., 2003; current version available at www.ggobi.org).

RESULTS

Gait and kinematic patterns

Approximately one-third of the sequences on the treadmill was recorded when the treadmill belt was not moving. As previous studies of mammalian locomotion have shown significant differences in kinematics between treadmill and overland walking (Alton et al., '98), a MANOVA was conducted on the angle variables measured to compare the conditions of belt-moving versus belt-stationary. No significant difference was detected (Wilks' $\lambda = 0.586$, $F = 0.724$, $P = 0.848$), perhaps because the mass of the newts is not large enough to cause deflection of the belt. Therefore, all terrestrial strides were pooled for subsequent analysis (Table 1).

TABLE 1. Summary of kinematic variables for level treadmill and underwater walking

	Environment	
Variable	Treadmill	Submerged
Angles		
Pectoral girdle range	23.54°	29.72
Pelvic girdle range	33.27°	44.43
Trunk range	55.22°	44.38
Minimum pectoral girdle–humerus	173.27°	161.65
Maximum pectoral girdle–humerus	216.73°	221.10
Minimum pelvic girdle–femur	144.75°	161.82
Maximum pelvic girdle–femur	204.47°	208.14
Minimum humerus–forearm	62.71°	97.73
Maximum humerus–forearm	147.34°	155.63
Minimum femur–crus	96.26°	116.08
Maximum femur–crus	159.31°	167.38
Minimum humerus–substrate	168.36°	156.35
Maximum humerus–substrate	201.12°	199.37
Minimum forearm–substrate	124.75°	132.93
Maximum forearm–substrate	170.75°	189.09
Minimum femur–substrate	169.39°	159.04
Maximum femur–substrate	207.24°	194.20
Minimum crus–substrate	136.07°	136.22
Maximum crus–substrate	179.16°	173.55
Time to		
Minimum pectoral girdle (%)	37.50	78.12
Maximum pectoral girdle (%)	85.55	10.88
Minimum pelvic girdle (%)	3.15	93.03
Maximum pelvic girdle (%)	55.81	46.44
Minimum trunk (%)	53.81	46.02
Maximum trunk (%)	4.25	97.88
Minimum pectoral girdle–humerus (%)	34.06	74.92
Maximum pectoral girdle–humerus (%)	8.45	17.47
Minimum pelvic girdle–femur (%)	93.77	78.78
Maximum pelvic girdle–femur (%)	64.69	23.50
Minimum humerus–forearm (%)	85.68	43.18
Maximum humerus–forearm (%)	6.70	85.10
Minimum femur–crus (%)	48.10	16.45
Maximum femur–crus (%)	95.99	88.04
Minimum humerus–substrate (%)	58.57	73.58
Maximum humerus–substrate (%)	33.90	19.41
Minimum forearm–substrate (%)	90.90	87.20
Maximum forearm–substrate (%)	44.87	38.67
Minimum femur–substrate (%)	86.59	19.13
Maximum femur–substrate (%)	76.47	82.02
Minimum crus–substrate (%)	42.59	12.08
Maximum crus–substrate (%)	87.24	82.74

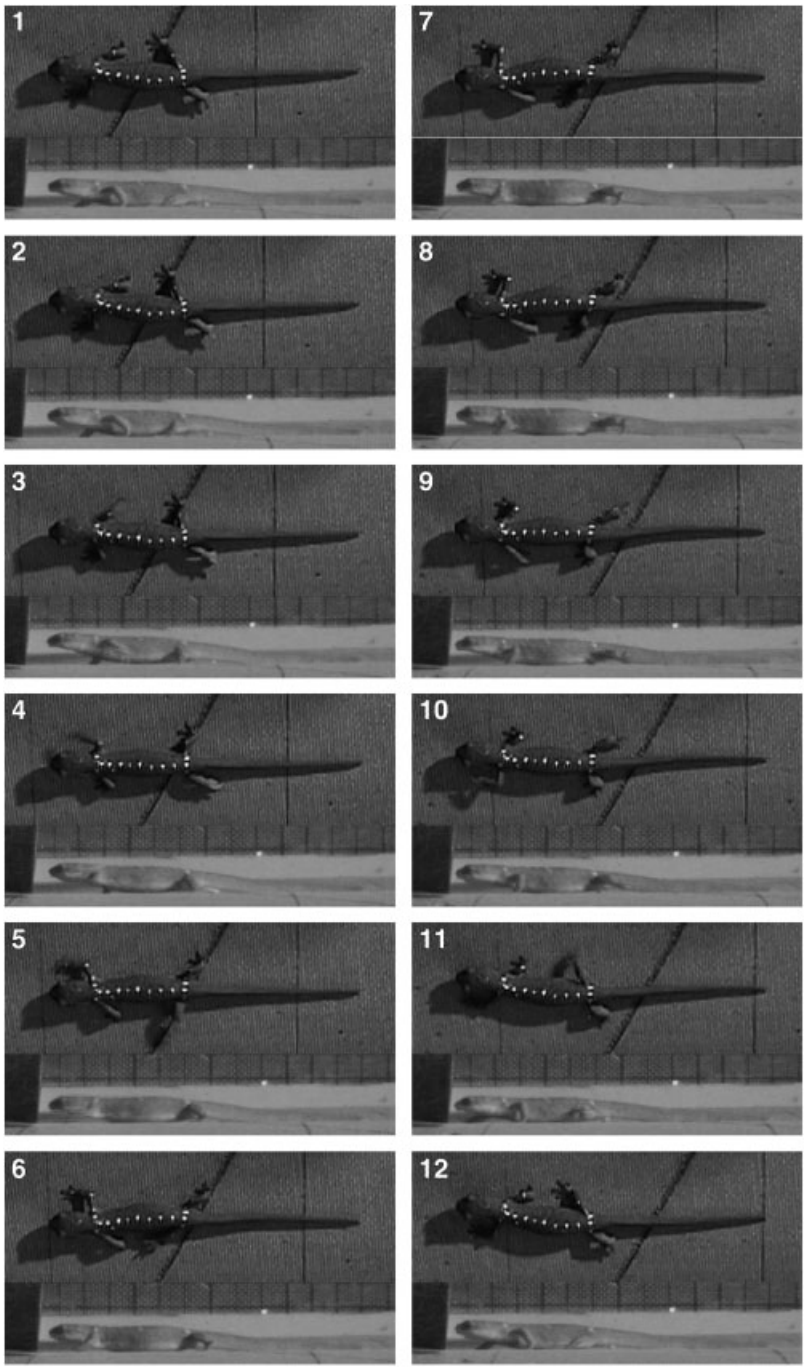

Fig. 1. Representative sequence of *Taricha* walking on a treadmill. Panels are in sequence from top to bottom, and are each separated in time by 100 msec. In each panel, top figure is a dorsal view, and bottom figure is a synchronous lateral view. In the dorsal view, the left side of the animal (the same side visible in the lateral view) is toward the top of the frame.

A representative stride showing *T. torosa* walking on the treadmill is shown in Figure 1, whereas a stride demonstrating submerged walking is shown in Figure 2. In both environments, lateral bending of the trunk in a standing wave pattern is evident, and movements of an individual limb are characterized by retraction throughout the stance phase followed by an elevated swing phase as the limb is lifted and protracted in preparation for the next stride (Figs. 1, 2).

Gait diagrams for both terrestrial and aquatic walking are shown in Figure 3. In terrestrial walking (upper panel in Figure 3), California newts use a gait that is classified as a slow

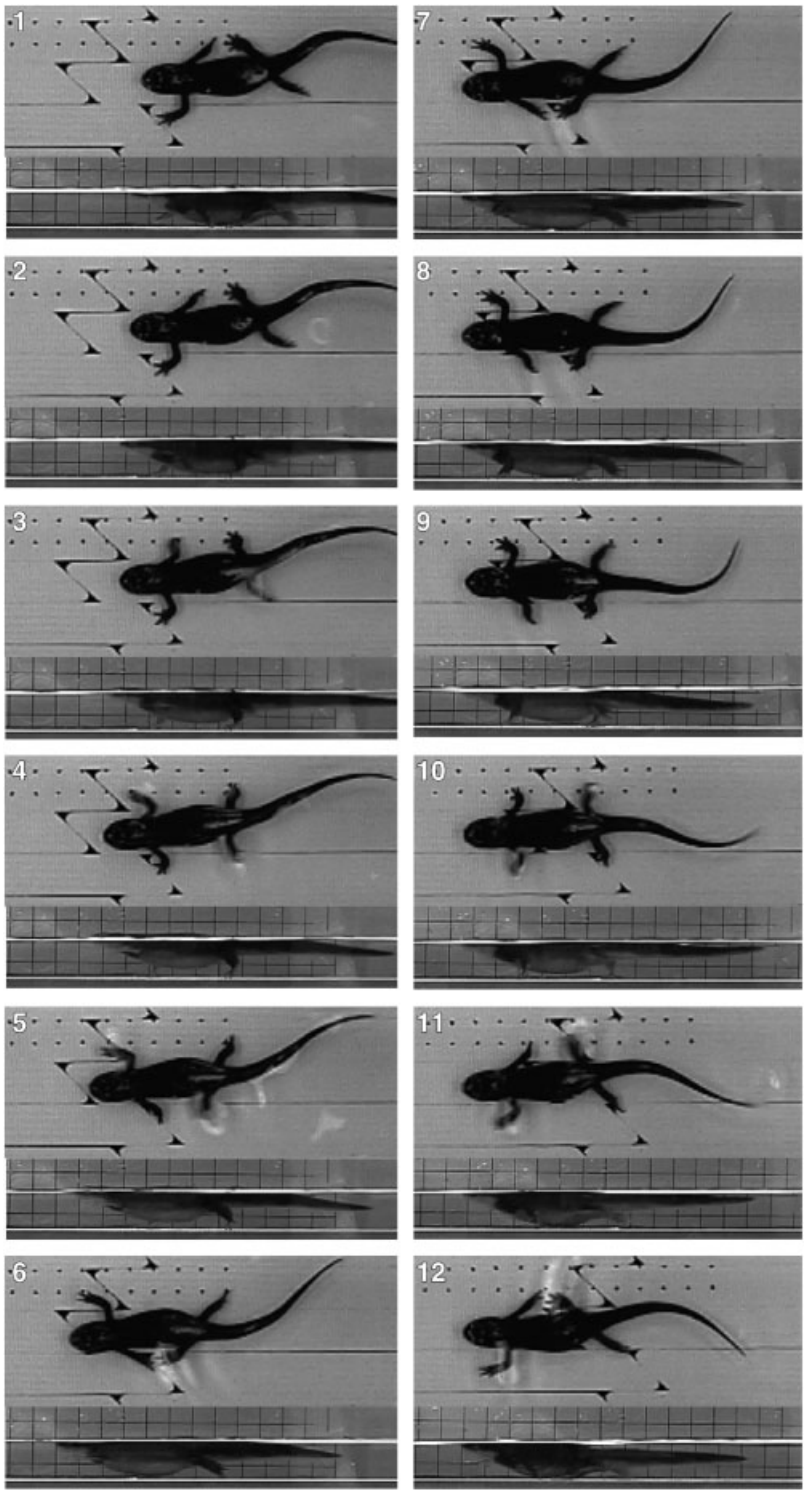

Fig. 2. Representative sequence of *Taricha* walking on a submerged trackway. Panels are in sequence from top to bottom, and are each separated in time by 100 msec. In each panel, top figure is a dorsal view, and bottom figure is a synchronous lateral view. In the dorsal view, the left side of the animal (the same side visible in the lateral view) is toward the top of the frame.

diagonal couplets lateral sequence walk (Hildebrand, '76; the first foot to fall after a given hindfoot is the forefoot on the same side of the body, and the footfalls of a diagonal limb pair [LH+RF, RH+LF] are closely spaced in time). Duty factor in terrestrial walking averages $77 \pm 3\%$ (Fig. 3),

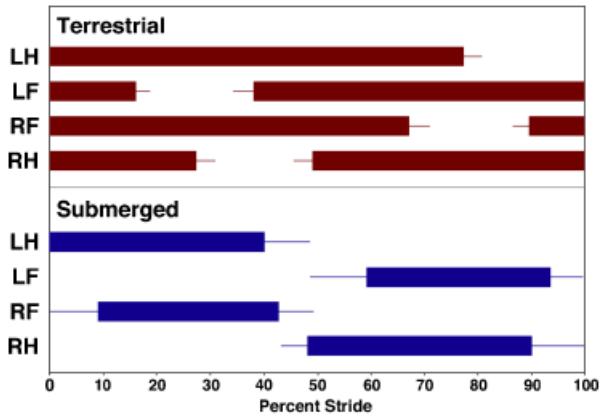

Fig. 3. Gait diagram for terrestrial and submerged locomotion in *Taricha*. Bars indicate periods during which the foot is on the ground; the ends of the bars are the mean times of foot placement/lift-off. Thin bars indicate one SD of foot placement or lifting. LH, left hindfoot; LF, left forefoot; RF, right forefoot; RH, right hindfoot. Upper panel: terrestrial walking. Average of 92 sequences. Lower panel: submerged walking. Average of 30 sequences.

stride length had a mean of 0.66 ± 0.09 SVL, and speed averaged 0.63 ± 0.13 SVL/sec (4.05 ± 0.54 cm/sec) in this study. There are periods of the stride (totaling approximately 24%, see Fig. 3) during which the newt is supported by only two (diagonally opposite) limbs, though the great majority of each stride sees the newt supported by three or even all four limbs. In contrast, during submerged strides, the duty factor is greatly reduced (mean of $41 \pm 8\%$; Fig. 3), stride length averaged 0.94 ± 0.24 SVL, and speed was nearly twice as great, with a mean of 1.19 ± 0.57 SVL/sec (7.85 ± 3.92 cm/sec). The underwater footfall pattern is altered such that it would be classified as a trot, although with a diagonal sequence (the first foot to fall after the left hindfoot is the forefoot on the opposite side of the body) rather than a lateral sequence, as has previously been shown in salamanders moving on land (Ashley-Ross, '94a). Unlike in terrestrial walking, there are periods of suspension when no limbs are in contact with the substrate (Fig. 3), a feature allowed only by the buoyant support of the water.

Mean kinematic profiles for the rotation of the limb girdles and overall bending of the trunk are shown in Figure 4. The pelvic girdle angle oscillates relatively smoothly around 90° (perpendicular to the direction of motion) in both terrestrial and submerged strides, though it shows a small but significant amount of phase advancement in submerged walking (Fig. 4, Table 2). The pectoral girdle angle is out of phase with the pelvic girdle angle in terrestrial walking, indicating that the two limb girdles are counter-rotating with respect to one another. Interestingly, the pectoral girdle angle shows less of a sinusoidal shape, reflecting the more varied, less stereotyped placements of the forefeet relative to the hindfeet. In submerged walking, the movements of the pectoral girdle are extremely variable (Fig. 4). The mean kinematic profile shows almost no pattern of side-to-side rotation; however, this profile shape is a result of the great amount of variation (note the large standard deviations for the pectoral girdle in submerged walking, Fig. 4). In contrast, the trunk angle oscillates symmetrically around 180° (trunk straight); the body axis assumes a standing wave pattern with nodes located at or close to the limb girdles (Figs. 1, 2, 4). As was the case for the pelvic girdle angle, the timing of trunk angle movement is slightly but significantly phase-advanced in submerged as compared with terrestrial walking (Table 2).

Average profiles for the angles between the limb girdles and the proximal limb segments (top panels in Fig. 5) show an asymmetry between the forelimb and hindlimb in both environments, in that the femur shows a more balanced amount of protraction and retraction (excursion to either side of 180°; hip angle) relative to the pelvic girdle, but the humerus shows an obviously greater amount of retraction relative to the pectoral girdle (values greater than 180°; shoulder angle) than protraction (Figs. 1, 5). In submerged strides, the range of motion is reduced for both limb segments; the femur is held nearly straight out from the pelvic girdle during the entire cycle (values hovering around 180°; Fig. 5). Note that in both environments the profiles are uniphasic, characterized by retraction during the entire stance phase, followed by protraction during the swing phase. Movements of both humerus and femur are in synchrony with girdle rotation, although there is a period surrounding the stance-swing transition when the segment angle remains steady before beginning protraction (Fig. 5).

If the humerus is not protracted relative to the line connecting the shoulder joints, then how is the forefoot placed anteriorly to begin the next stride? An examination of Figures 1 and 2 reveals that the forelimb and hindlimb are fundamentally different in their internal movements. The advance of the hindlimb is owing to a combination of the pelvic girdle swinging forward on that side and protraction of the femur. The forelimb, in contrast, shows little oscillation of the pectoral girdle,

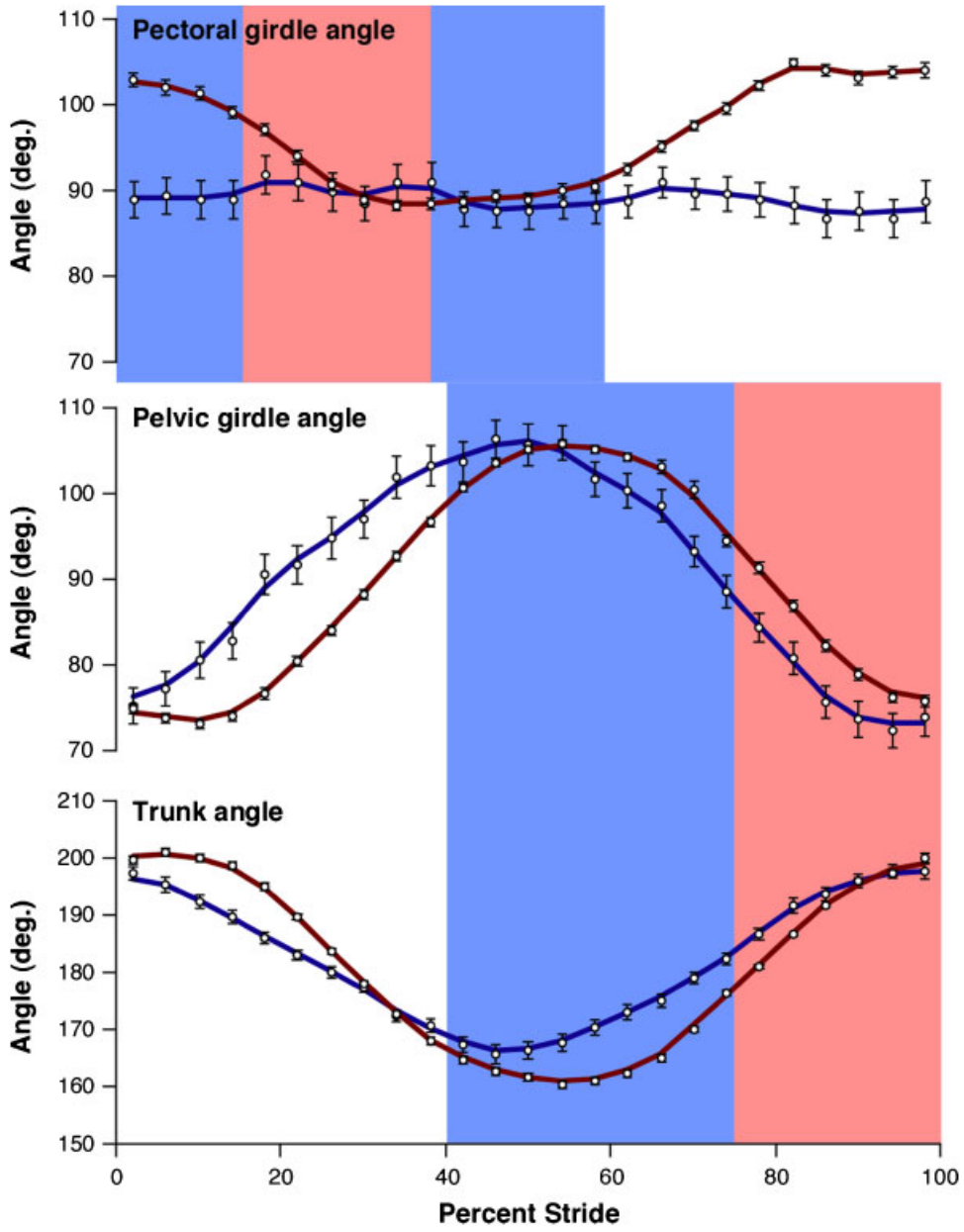

Fig. 4. Average kinematic profiles of two-dimensional pectoral girdle (top panel), pelvic girdle (middle panel), and overall trunk (bottom panel) angles for terrestrial (red line) and aquatic (blue line) walking. Symbols indicate mean values; error bars are SD. The solid lines are twice-smoothed averages, presented solely to show the overall shape of the traces (not used to calculate angle minima and maxima). The shaded region indicates the swing phase of the stride; the red region corresponds to the terrestrial stride, whereas the shaded blue region plus the shaded red region indicate the swing phase of the aquatic stride.

and little protraction of the humerus. Instead, placement of the foot far anterior to the shoulder joint is principally because of flexion of the elbow joint. The bottom traces in Figure 5 illustrate the mean kinematic profiles for the three-dimensional angles between the humerus and forearm (elbow angle) and the femur and crus (knee angle). Consideration of these traces in conjunction with those in the upper panels supports the distinction between forelimb and hindlimb kinematics. For both terrestrial and submerged strides, the knee joint begins to flex immediately as soon as the foot comes in contact with the substrate, continuing this motion until approximately one-half of the way through the stance phase. Flexion of the knee coincides with femoral retraction, indicating that the body is being pulled toward the foot during this period (approximately the first quarter of the

TABLE 2. Individual ANOVA results for kinematic angle and timing variables comparing environment (same as in Table 1) and individual

	Environment (df = 1)		Individual (df = 2)	
Variable	*F*	*P*	*F*	*P*
Angles				
Pectoral girdle range	1.274	0.3761	9.977	**0.0003**
Pelvic girdle range	2.197	0.2765	1.198	0.3119
Trunk range	1.201	0.3875	25.204	**0.0001**
Minimum pectoral girdle–humerus	1.540	0.3404	4.074	0.0242
Maximum pectoral girdle-humerus	0.1560	0.7309	21.528	**0.0001**
Minimum pelvic girdle–femur	3.005	0.2251	39.419	**0.0001**
Maximum pelvic girdle–femur	21.182	0.0441	18.840	**0.0001**
Minimum humerus–forearm	3.312	0.2104	22.294	**0.0001**
Maximum humerus–forearm	31.556	0.0303	1.505	0.2337
Minimum femur–crus	0.711	0.4879	59.378	**0.0001**
Maximum femur–crus	0.008	0.9979	13.689	**0.0001**
Minimum humerus–substrate	6.760	0.1215	22.486	**0.0001**
Maximum humerus–substrate	2.225	0.2743	39.580	**0.0001**
Minimum forearm–substrate	0.446	0.5728	19.764	**0.0001**
Maximum forearm–substrate	8.014	0.1054	4.260	0.0207
Minimum femur–substrate	32.917	0.0291	5.394	0.0082
Maximum femur–substrate	2.306	0.2682	63.429	**0.0001**
Minimum crus–substrate	0.100	0.7814	91.395	**0.0001**
Maximum crus–substrate	1.446	0.3522	0.532	0.5915
Time to				
Minimum pectoral girdle	15.358	0.0594	1.928	0.1581
Maximum pectoral girdle	22.571	0.0416	3.343	0.0449
Minimum pelvic girdle	607.718	**0.0016**	0.995	0.3783
Maximum pelvic girdle	7.958	0.1060	0.037	0.9637
Minimum trunk	562.000	**0.0018**	12.886	**0.0001**
Maximum trunk	2,172.000	**0.0005**	0.153	0.8585
Minimum pectoral girdle–humerus	12.669	0.0707	7.873	**0.0012**
Maximum pectoral girdle–humerus	2.127	0.2821	6.201	0.0044
Minimum pelvic girdle–femur	1.633	0.3295	18.709	**0.0001**
Maximum pelvic girdle–femur	8.196	0.1034	6.086	0.0048
Minimum humerus–forearm	0.698	0.4914	1.797	0.1784
Maximum humerus–forearm	22.637	0.0414	1.853	0.1693
Minimum femur–crus	31.442	0.0304	1.938	0.1566
Maximum femur–crus	21.164	0.0441	0.545	0.5837
Minimum humerus–substrate	4.557	0.1663	8.089	**0.0011**
Maximum humerus–substrate	0.008	0.9364	1.164	0.3221
Minimum forearm–substrate	0.195	0.7018	1.197	0.3122
Maximum forearm–substrate	2.904	0.2305	0.249	0.7811
Minimum femur–substrate	4.799	0.1599	0.285	0.7532
Maximum femur–substrate	0.199	0.6989	1.135	0.3311
Minimum crus–substrate	46.982	0.0206	1.559	0.2223
Maximum crus–substrate	0.335	0.6210	1.357	0.2685

Bold type indicates a significantly difference at $\alpha = 0.05$ (sequential Bonferroni-corrected).

step cycle); maximum knee flexion does not reach 90° (Fig. 5, lower right panel). Knee extension occurs throughout the remainder of stance phase, until the foot has rolled up on the toes and the ankle has started moving forward preparatory to lifting of the foot (Figs. 1, 2, 5). The swing phase is marked by initial flexion of the knee, followed by extension as the foot is brought into position for the start of the next stride. Although the range of motion is reduced and the overall knee angle is more extended in submerged walking, the same pattern is nonetheless present. The elbow joint, like the knee, shows a biphasic pattern, but the amount of extension and flexion in early stance is small. It undergoes only slight extension followed by minimal flexion again for approximately the

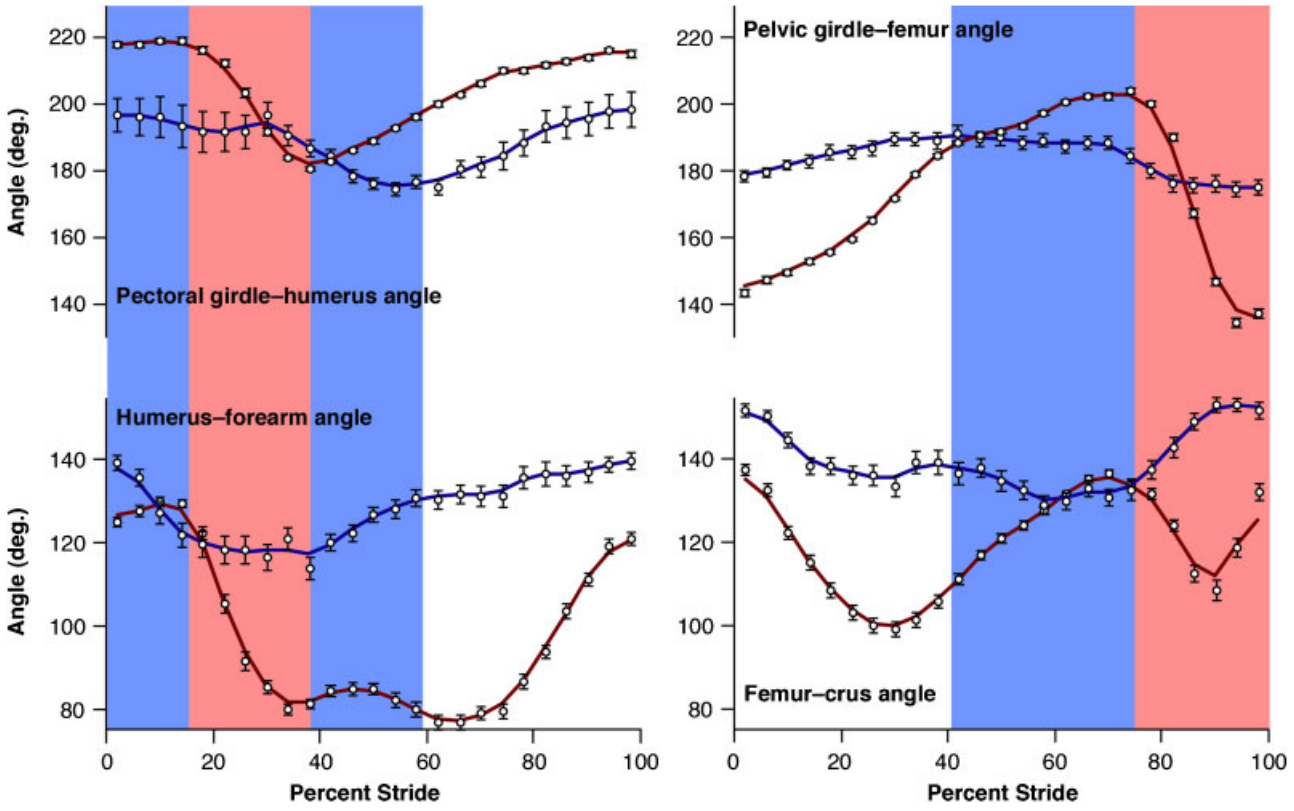

Fig. 5. Average kinematic profiles of two-dimensional angles between the pectoral girdle and humerus (upper left), and between the pelvic girdle and femur (upper right), and three-dimensional angles between the humerus and forearm (lower left) and between the femur and crus (lower right) for terrestrial and aquatic walking. Symbols and colors are as in Figure 4.

first quarter of the forefoot stance phase, after which it extends for the remainder of stance. The majority of flexion occurs during swing in both environments (Figs. 1, 2, 5).

It is interesting to note the differences between the movement patterns of the forelimb and hindlimb; the hindfeet are placed in advance of the hip joint primarily owing to femoral protraction, whereas the forefeet owe their placement on the substrate in a position anterior to the shoulder joint to elbow flexion, as the humerus does not undergo a great deal of protraction (Fig. 5). The most obvious difference for knee and elbow joint movement patterns in submerged walking is that both are shifted to more extended angles for nearly the entire stride (Fig. 5, bottom panels).

Figure 6 shows the average profiles for the three-dimensional angles between the limb segments (humerus, femur, forearm, and crus) and the substrate surface. For all four of these angles, a value of 180° indicates that the limb segment is parallel to the substrate surface. In terrestrial walking, the proximal limb segments have values greater than 180° for most of the stride, indicating that the distal end is higher than the proximal end. Thus, the newt is suspended in the middle of the sprawled limbs. The distal limb segments, not unexpectedly (as the feet spend most of the stride on the ground), show values less than 180° for most of the stride. Even during the swing phases of the forelimb and hindlimb, the average values do not exceed 180°. Thus, the feet are not lifted far off the substrate during the swing phase of the limb; the elevation of the distal ends of the humerus and femur are counteracted by the depression of the distal ends of the forearm and crus (Figs. 1, 6). In submerged strides, the humerus and femur are held in more depressed positions, and the forearm makes a more obtuse angle with the substrate, than in terrestrial walking (Figs. 2, 6). To gauge the degree to which the limbs are depressed in water, we measured the maximum absolute vertical distance between the dorsal edge of the sacrum and the ankle joint. For terrestrial strides, this value averaged 0.78 ± 0.21 cm; for submerged strides, the maximum vertical distance was 1.11 ± 0.17 cm. Thus, the body weight of the newt is at least partially

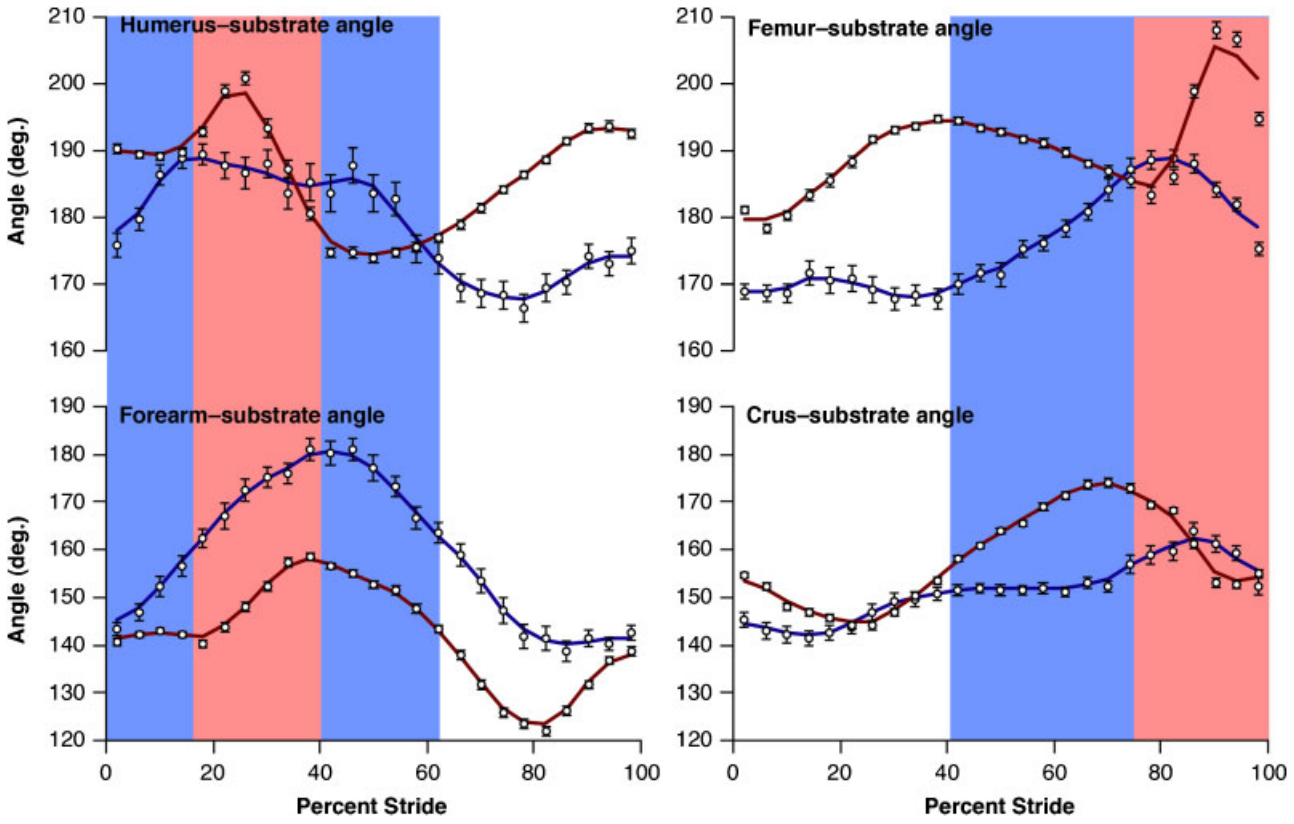

Fig. 6. Average kinematic profiles of three-dimensional angles between the indicated limb segment and substrate surface for terrestrial and aquatic walking. Upper left panel, humerus. Upper right panel, femur. Lower left panel, forearm. Lower right panel, crus. Symbols and colors are as in Figure 4.

supported by the buoyancy of the water, allowing the four limbs to project down as well as laterally.

DISCUSSION

Effect of smoothing on kinematic data

A concern that often arises in kinematic studies is the reliability of the data, based as it is on the manual tracking of points in video frames. Error in selecting the position of anatomical markers introduces error into subsequent calculations of kinematic parameters. Smoothing the raw data by various methods (e.g., de Lange et al., '90; Vint and Hinrichs, '96; Rosenhahn et al., 2007) is typically used to reduce digitizing error. However, it is possible that smoothing the data may dampen the true amplitude of angular minima and maxima. We, therefore, compared the average kinematic traces for the smoothed data versus the raw data; four representative plots for terrestrial walking are shown in Figure 7. The variables chosen show that for both two-dimensional angles (trunk angle, pelvic girdle–femur angle) and three-dimensional angles (femur–crus angle, crus–substrate angle), the smoothed profiles closely approximate the raw averages, and the effect of ''clipping'' peaks is minimal. Additionally, the effect of smoothing should be the same for both terrestrial and underwater walking, and thus should not introduce any bias that would alter statistical comparisons. We, therefore, argue that the smoothed data are an accurate representation of the true kinematic parameters for walking.

Hydrodynamics of underwater walking: the effect of environment

The results of this study support the predictions of the reduced-gravity model of walking (He et al., '91; Martinez et al., '98): in comparison to terrestrial strides, underwater walking is characterized by shorter duty factors (Fig. 3) and greater variability in kinematics (Figs. 4–6), because of reduced constraints on support because of buoyancy. An indicator of the effect of buoyant support on variability is the extent of vertical movements of the pelvic girdle in both environments. Over the course of a terrestrial stride, the pelvic girdle moves up and down by an average of

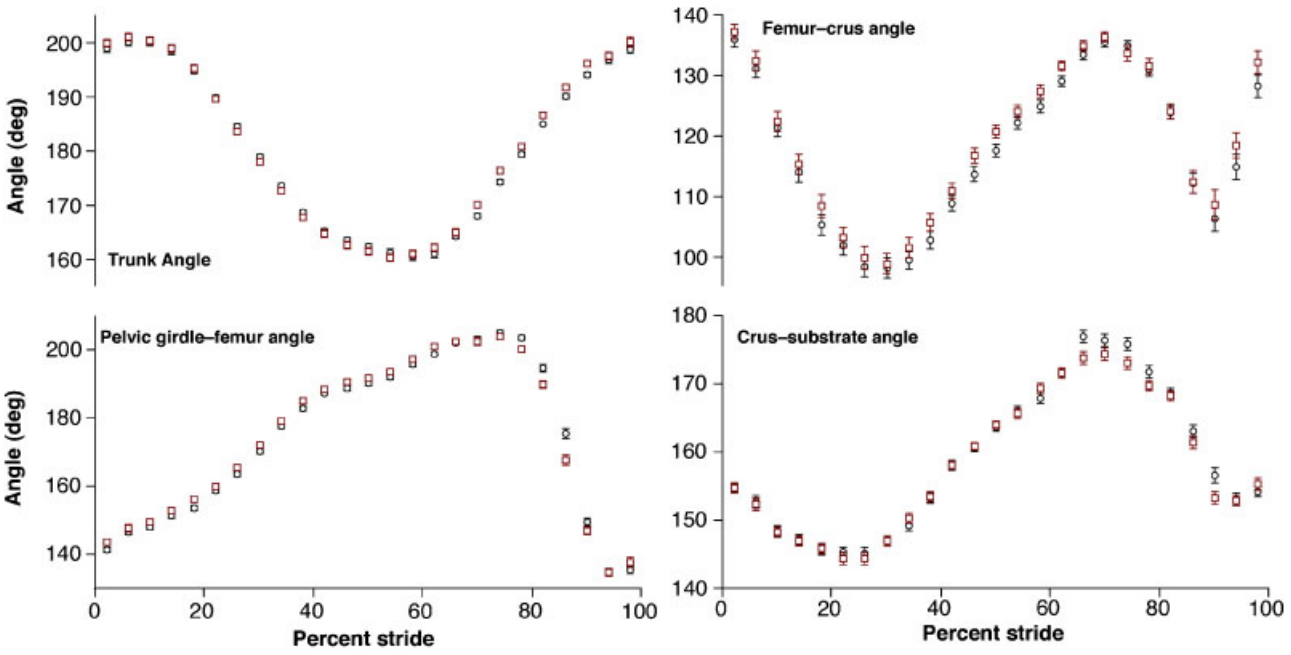

Fig. 7. Comparison of kinematic profiles based on the averages of the raw data (black symbols) and smoothed data (red symbols) for four representative variables in terrestrial walking. Symbols indicate mean values; error bars are SD.

0.35 ± 0.33 cm; in underwater walking, the corresponding value is 0.52 ± 0.22 cm. Therefore, we conclude that a portion of the greater variability seen in underwater kinematics is owing to larger vertical movements of the newt's body. However, not all variation can be ascribed to this cause; timing of limb movements, in particular, is unlikely to be substantially affected. Instead, we suggest that the greater density and viscosity of water plays a central role in determining the timing of gross limb movements. A salamander moving through water must contend with the force of drag, which acts to resist forward motion (Vogel, '94, 2003). Additionally, because walking in any environment necessarily involves repetitive acceleration and deceleration of the limbs, submerged walkers must deal with the acceleration reaction force (Martinez, '96, 2001). This force has components owing to the acceleration of the limb itself, and also of the water that behaves as though it were being dragged in lockstep with the limb. Drag is dependent on the square of velocity, whereas the acceleration reaction force scales directly with velocity (Martinez, '96). Thus, we can expect the newt to act to minimize these detrimental forces by reducing the velocity of the limbs as they are being swung forward through the water. Reduced duty factor and the shift toward a trotting gait pattern, means that the limbs are spending more absolute time (over twice as long) in the swing phase than they would if submerged walking followed the same lateral sequence pattern seen on land. If submerged walkers used the same footfall pattern as on land, the acceleration reaction force during early swing would be twice as great, and drag four times as great, as what the newt contends with by shifting to the more trot-like gait. The duration of the swing phase is extended further by the periods of suspension, when no limbs are in contact with the substrate (an event never seen in terrestrial locomotion). Thus, buoyant support also contributes to drag-reducing features of the underwater stride.

Interlimb and limb–axial coordination

Movement patterns of the limbs and body are highly regular during walking in *Taricha*, though, as hypothesized, more variable when submerged than when on land. Forward swings of individual limbs are associated with the advance of the corresponding side of the limb girdle, and with lateral flexion that serves to also advance the limb (Figs. 1, 2, 4, 5). Thus, axial and limb movements are tightly coupled, as has been shown for terrestrial walking in other salamanders (e.g., Daan and Belterman, '68; Frolich and Biewener, '92) and some lizards (Ritter, '92; Ashley-Ross, '94a), as well as in larval zebrafish (coupled

movements of the pectoral fins and axial structures; Budick and O'Malley, 2000; Müller and van Leeuwen, 2004; Thorsen et al., 2004), swimming coelacanth (Fricke and Hissmann, '92), and epaulette sharks walking underwater (Pridmore, '94). The footfalls of the diagonal limb pairs are tightly coupled (Fig. 3), although there is a fundamental shift in footfall pattern in the two environments, such that what was a lateral sequence walk on land becomes a diagonal sequence trot in water. As predicted, the proportion of the stride occupied by the stance and swing phases is altered. On land, slightly over three-quarters of the stride is spent with the foot in contact with the ground, with the result that the hip on that side has begun moving forward before the associated limb swings forward. In water, the movements of the limb and hip are more closely synchronized. In both environments, though the diagonal limbs are moving forward, the trunk is flexing so that it is concave toward the side of the advancing hindlimb (Figs. 1, 2, 4, 5). The rotation of the pelvic girdle is of greater amplitude, and more smoothly sinusoidal, than that of the pectoral girdle (Fig. 4); this may reflect the role of the forelimbs in setting the direction of travel of the newt, or may merely be a consequence of a necessity to keep the head pointing forward without excessive side-to-side swinging. Rotation of the limb girdle that would move the shoulder/hip joint posteriorly is coincident with retraction of the associated limb (Figs. 4, 5, upper panels). In terrestrial walking, both the pectoral and pelvic girdles have begun rotating back to their original orientation before the associated limb is lifted to begin its swing phase. In submerged walking, the change in direction of oscillation of the limb girdles is more co-incident with the beginning of the swing phase of the associated limb (Fig. 4), a feature reminiscent of the coordinated movements of the pectoral fin and body axis in larval zebrafish (Thorsen et al., 2004). Previous authors (Daan and Belterman, '68; Edwards, '77) have suggested that terrestrial locomotion may have originally been accomplished by combining traveling waves of axial undulation with the support of limbs used simply as rigid pegs to prevent slippage. Such a hypothesis does not offer a compelling explanation for how complex movement patterns of the limb segments arose. Indeed, several authors have shown that in elongate forms, tetrapods *lose* the strict coordination between limbs and axial structures (Renous et al., '99; Azizi and Horton, 2004). Interestingly, Thorsen et al. (2004) have suggested that the tight coupling of alternating fin/limb movements with body axis oscillation seen in larval zebrafish may represent the retention of a larval neural program for use in a new context, namely, limb-based locomotion. Similar tight coupling that has been shown in this study to characterize underwater walking in newts offers further support to the idea that the neural circuitry supporting walking patterns in early tetrapods is evolutionarily ancient.

Kinematics of terrestrial versus submerged walking

Given the similarities and differences in individual angles between submerged and terrestrial strides noted above, one might reasonably ask the question, ''Is underwater walking fundamentally different from walking on land?'' There is no question that the footfall pattern is different, being shifted from a lateral sequence walk with a duty factor of 77% to a diagonal sequence gait with a duty factor of only 41%; we have argued above that the change in footfall pattern can be ascribed to hydrodynamic forces. Do those shifts in footfall timing and duty factor necessitate a substantial change in limb kinematics, or do the limbs move in more or less the same way regardless of the medium through which they are moving? We were particularly interested in the relative timing of limb movements, as these represent shifts from one set of active muscles to another (and therefore may reflect the basic motor pattern). In order to make visual comparison of the shapes of the traces for the two environments easier, the average profiles for the limb angles were transformed to fit an idealized stride composed of 50% stance and 50% swing. Likewise, to remove the confounding effects of different (or shifted) angle ranges, they were plotted as a percent of the total excursion range. These idealized plots are shown in Figures 8 and 9. When standardized to the basic events of the stride (stance and swing), it is evident that the hip and shoulder joints are moving in highly similar manners (upper panels in Fig. 8). Likewise, the basic patterns of the elbow and knee joints appear to be conserved, with peaks of extension centered around the transitions between stance and swing phases, and valleys of flexion in the middle of the stance and swing phases (lower panels in Fig. 8). Idealized plots of the individual limb segments with the substrate likewise show considerable shape similarity between the two environments (Fig. 9). The only

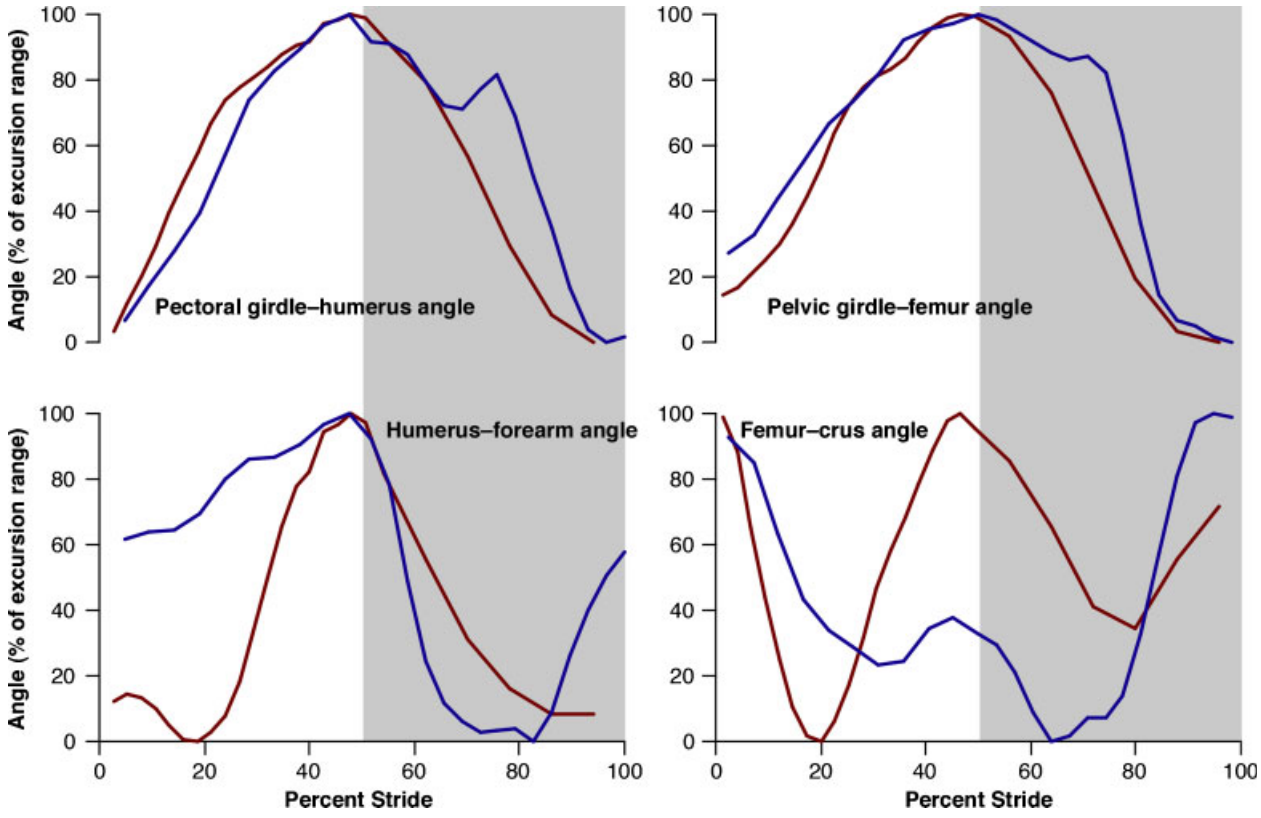

Fig. 8. Standardized kinematic profiles of the indicated angles for terrestrial and aquatic walking. Values were transformed so that the stride was composed of 50% stance and 50% swing phase, and angles were plotted as percent of the excursion range. Upper left panel, two-dimensional pectoral girdle–humerus angle. Upper right panel, two-dimensional pelvic girdle–femur angle. Lower left panel, three-dimensional humerus–forearm angle. Lower right panel, three-dimensional femur–crus angle. Colors are as in Figure 4.

variable that shows a real shape difference is the knee angle during the swing phase (Fig. 9, lower right panel); the terrestrial profile is characterized by a large amount of flexion for most of the swing, whereas the submerged trace shows extension during the corresponding period.

Considering all angle variables together in a MANOVA demonstrates significant difference between terrestrial and submerged walking (Wilks' $\lambda = 0.008$, $F = 236.2$, $P < 0.001$). However, few individual variables showed significant difference between the two environments. When corrected for multiple comparisons (Rice, '89), only three variables, all relating to the timing of trunk and pelvic girdle movements, were statistically significant (time to minimum pelvic girdle angle, $F_{1,2} = 607$, $P = 0.001$; time to minimum trunk angle, $F_{1,2} = 562$, $P = 0.001$; time to maximum trunk angle, $F_{1,2} = 2172$, $P = 0.0005$). However, the conservatism resulting from the sequential Bonferroni correction may mask real differences between the kinematics in the two environments.

An alternative way to explore the data is to use visualization programs developed for multidimensional data, such as Ggobi. Plotting all of the angular variables simultaneously, Ggobi allows one to take a "tour" of the data as it animates the data clouds to reflect changing axes for the two-dimensional plots. Two freeze-frames from that tour are shown in Figure 10, representing the extremes of the data set. Most of the tour resembles that in the upper panel, with complete overlap between terrestrial and submerged strides. Only one configuration, shown in the lower panel, separates the clouds of points for the two environments (Fig. 10). The axes of separation are those that were significant in the ANOVAs (timing of minima/maxima in pelvic girdle and trunk angles). The full animated tour is available for viewing at http://www.wfu.edu/~rossma/newttour.html. Lack of separation for the vast majority of the configurations of data clouds in the tour reinforces the idea that there is a fundamental kinematic pattern for walking, that

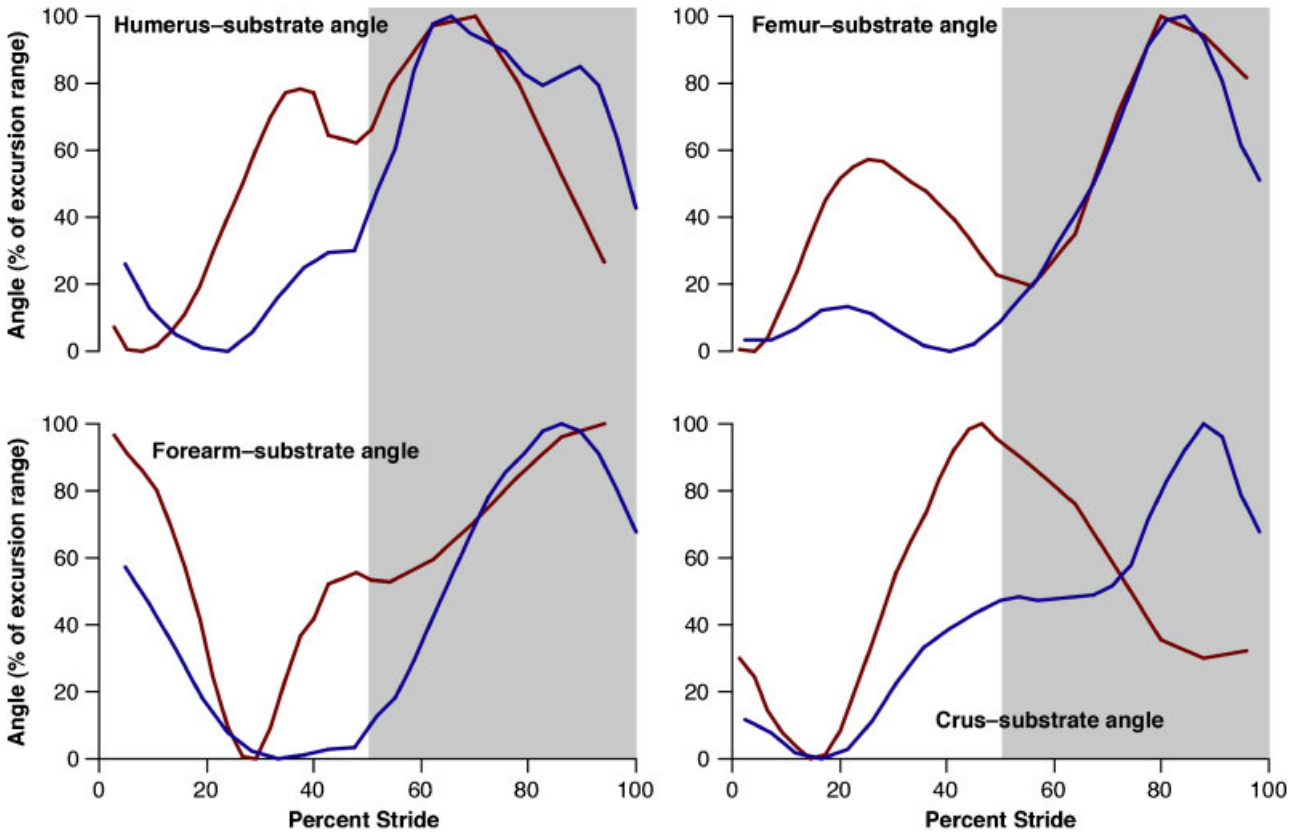

Fig. 9. Standardized kinematic profiles of three-dimensional angles between the indicated limb segment and substrate surface for terrestrial and aquatic walking. Values were transformed so that the stride was composed of 50% stance and 50% swing phase, and angles were plotted as percent of the excursion range. Upper left panel, humerus. Upper right panel, femur. Lower left panel, forearm. Lower right panel, crus. Colors are as in Figure 4.

is used regardless of the environment with only slight changes necessary.

Comparison with kinematics of level walking in Dicamptodon and other tetrapods

During treadmill walking, *Taricha* uses a lateral sequence walk, the gait that is most widespread among tetrapod groups (Hildebrand, '76). The duty factor and phase relationships among the limbs in this study were similar to those seen for walking *Dicamptodon*, though relative stride length was slightly shorter (0.66 SVL/stride in *Taricha* versus 0.73 SVL/stride in *Dicamptodon*; Ashley-Ross, '94a). Pelvic girdle and trunk angle ranges were similar to *Dicamptodon* as well; Ashley-Ross ('94a) found pelvic girdle rotation of 38.5° and trunk flexion of 65.7°, which are values slightly larger than shown by *Taricha* (33.3 and 55.2°, respectively). Protraction and retraction of the femur were more extensive in *Dicamptodon* (minimum and maximum angles of 129 and 235°, respectively; compared with values in Table 1). Numerical comparison of other angle values given in Ashley-Ross ('94a) is inappropriate, as the values given there for femur–crus angle and the angle between the crus and the treadmill surface were two-dimensional. Nonetheless, similarity is evident in the shape of the kinematic profiles for pelvic girdle angle, trunk angle, pelvic girdle–femur angle, and femur–crus angle (compare Fig. 4 in Ashley-Ross, '94a).

Direct comparison of hindlimb kinematics in the California newt with other tetrapod taxa is challenging, because of differences in gaits and speed. However, for studies where a sprawling, lateral sequence walk was employed, some similarities are evident. First, lateral flexion of the trunk in a standing wave pattern with nodes close to the limb girdles is a common feature, seen in *Alligator* (Reilly and Elias, '98), *Caiman* (Brinkman, '80), and *Iguana* (Brinkman, '81). Even in primitive mammals, this characteristic is evident (e.g., *Monodelphis*; Pridmore, '92). Pelvic girdle rotation is coordinated with trunk flexion; the range of motion

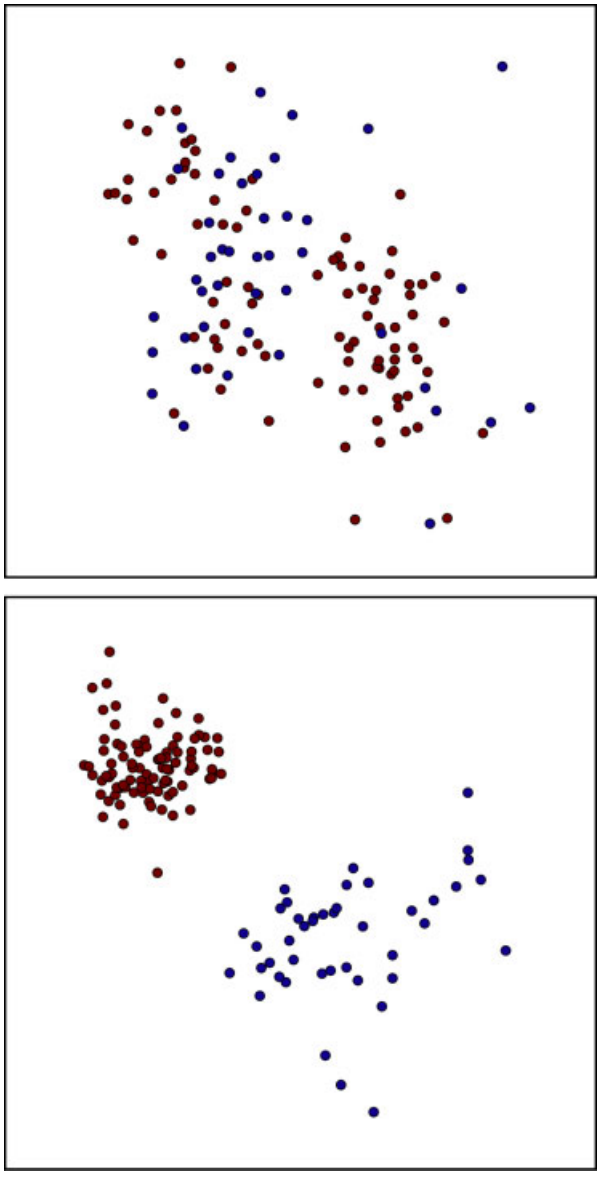

Fig. 10. Two-dimensional projections of Ggobi multidimensional data tour, where all variables were plotted simultaneously in multidimensional space. Upper panel illustrates that for most of the time, terrestrial and submerged strides were not separable. Lower panel illustrates that when the data cloud was in a few select projections, it is possible to separate terrestrial from submerged strides. A QuickTime movie of the data tour is available at http://www.wfu.edu/~rossma/newttour.html. Colors are as in Figure 4.

may be smaller (e.g., 26° in *Alligator*: Reilly and Elias, '98) or similar to (41° in *Caiman*: Brinkman, '80; 30° in *Iguana*: Brinkman, '81; 30–40° in *Monodelphis*: Pridmore, '92) that of *Taricha*. Femoral retraction beginning immediately at footfall and persisting through stance is also a common feature, though again the angular values may differ. Reilly and Elias ('98) noted a smaller range of motion of the femur (approximately 40°); however, Blob and Biewener (2001) show a range of approximately 90° in *Alligator* moving at a faster speed. *Caiman* had a range of femoral motion of 48° (Brinkman, '80), whereas *Iguana* showed a much larger amount of protraction and retraction of the femur (70–118°; Brinkman, '81; Blob and Biewener, 2001). Although the knee joint angles cannot be compared (two-dimensional versus three-dimensional angles), the kinematic profiles nonetheless show the same general features of initial flexion in early stance, followed by extension for the remainder of the stance phase (though Reilly and Elias, '98, describe a pattern of slight flexion followed by near-stasis of the knee joint throughout much of stance). These features of the step cycle have previously been proposed to be plesiomorphic for tetrapods (Ashley-Ross, '94a); it is unsurprising, though heartening, to find that *Taricha* shares these characteristics.

Conclusions: submerged walking and the water-to-land transition

In this study, we have demonstrated that terrestrial and submerged walking are significantly different from one another, with the gait pattern used being driven by the environment. Limb–axial coordination in submerged walking is similar to the patterns previously described for underwater walking in sharks (Pridmore, '94) and slow swimming in larval zebrafish (Thorsen et al., 2004) and coelacanth (Fricke and Hissmann, '92), as well as to terrestrial trots in quadrupeds. We have also shown that the timings of kinematic events in both environments are broadly conserved, with reversals of joint movements occurring at similar points in the step cycle. Finally, we have illustrated basic similarities in features of the step cycle for the level lateral sequence walk among various sprawling tetrapods. Taken collectively, these observations suggest that the basic pattern of walking is evolutionarily quite ancient; as Thorsen et al. (2004) have suggested, it is possible that the earliest tetrapod ancestors made use of neural circuits used for larval fish locomotion, neotenically retained and co-opted for underwater walking, and finally applied with minimal changes to terrestrial locomotion. Research on the motor patterns controlling walking both in and out of the water and the transitions between environments, is sorely needed to test these ideas regarding the evolution of tetrapod locomotion.

ACKNOWLEDGMENT

We thank Alistair Cullum for making Didge available for kinematic analysis. Supported by a National Science Foundation grant (IBN 0316331) to M.A.-R. We also thank two anonymous reviewers, whose thoughtful comments greatly improved the study.

LITERATURE CITED

Alton F, Baldey L, Caplan S, Morrissey MC. 1998. A kinematic comparison of overground and treadmill walking. Clin Biomech 13:434–440.

Ashley-Ross MA. 1994a. Hind limb kinematics during terrestrial locomotion in a salamander (*Dicamptodon tenebrosus*). J Exp Biol 193:255–283.

Ashley-Ross MA. 1994b. Metamorphic and speed effects on hind limb kinematics during terrestrial locomotion in the salamander *Dicamptodon tenebrosus*. J Exp Biol 193: 285–305.

Ashley-Ross MA. 1995. Patterns of hind limb motor output during walking in the salamander *Dicamptodon tenebrosus*, with comparisons to other tetrapods. J Comp Physiol A 177:273–285.

Ashley-Ross MA, Bechtel BF. 2004. Kinematics of the transition between aquatic and terrestrial locomotion in the newt *Taricha torosa*. J Exp Biol 207:461–474.

Azizi E, Horton JM. 2004. Patterns of axial and appendicular movements during aquatic walking in the salamander, *Siren lacertina*. Zool Anal Complex Syst 107:111–120.

Biewener AA. 1998. Muscle–tendon stresses and elastic energy storage during locomotion in the horse. Comp Biochem Physiol B 120:73–87.

Blob RW, Biewener AA. 2001. Mechanics of limb bone loading during terrestrial locomotion in the green iguana (*Iguana iguana*) and American alligator (*Alligator mississippiensis*). J Exp Biol 204:1099–1122.

Breithaupt R, Dahnke J, Zahedi K, Hertzberg J, Pasemann F. 2002. Robo-Salamander: an approach for the benefit of both robotics and biology. In: Bedaud P, editor. Fifth international conference on climbing and walking robots. Paris, France. p 55–62.

Brinkman D. 1980. The hind limb step cycle of *Caiman* sclerops and the mechanics of the crocodile tarsus and metatarsus. Can J Zool 58:2187–2200.

Brinkman D. 1981. The hind limb step cycle of *Iguana* and primitive reptiles. J Zool Lond 181:91–103.

Budick SA, O'Malley DM. 2000. Locomotor repertoire of the larval zebrafish: swimming, turning and prey capture. J Exp Biol 203:2565–2579.

Daan S, Belterman T. 1968. Lateral bending in the locomotion of some lower tetrapods. Proc Ned Akad Wetten C 71:245–266.

de Lange A, Huiskes R, Kauer JMG. 1990. Effects of data smoothing on the reconstruction of helical axis parameters in human joint kinematics. J Biomech Eng 112:107–113.

Delvolve I, Bem T, Cabelguen J-M. 1997. Epaxial and limb muscle activity during swimming and terrestrial stepping in the adult newt, *Pleurodeles waltl*. J Neurophysiol 78:638–650.

Deuel NR, Park J. 1993. Gallop kinematics of Olympic three-day event horses. Acta Anat 146:168–174.

Dowis HJ, Sepulveda CA, Graham JB, Dickson KA. 2003. Swimming performance studies on the eastern Pacific bonito *Sarda chiliensis*, a close relative of the tunas (family Scombridae) II. Kinematics. J Exp Biol. 206:2749–2758.

Edwards JL. 1977. The evolution of terrestrial locomotion. In: Hecht MK, Goody PC, Hecht BM, editors. Major patterns in vertebrate evolution. New York: Plenum Publishing Corp. p 553–576.

Edwards JL. 1989. Two perspectives on the evolution of the tetrapod limb. Am Zool 29:235–254.

Ellerby DJ, Spierts ILY, Altringham JD. 2001. Fast muscle function in the European eel (*Anguilla anguilla L.*) during aquatic and terrestrial locomotion. J Exp Biol 204:2231–2238.

Fish FE. 1998. Comparative kinematics and hydrodynamics of odontocete cetaceans: morphological and ecological correlates with swimming performance. J Exp Biol 201: 2867–2877.

Fish FE. 2000. Biomechanics and energetics in aquatic and semiaquatic mammals: platypus to whale. Physiol Biochem Zool 73:683–698.

Fish FE, Baudinette RV. 1999. Energetics of locomotion by the Australian water rat (*Hydromys chrysogaster*): a comparison of swimming and running in a semi-aquatic mammal. J Exp Biol 202:353–363.

Fricke H, Hissmann K. 1992. Locomotion, fin coordination and body form of the living coelacanth *Latimeria chalumnae*. Environ Biol Fish 34:329–356.

Frolich LM, Biewener AA. 1992. Kinematic and electromyographic analysis of the functional role of the body axis during terrestrial and aquatic locomotion in the salamander *Ambystoma tigrinum*. J Exp Biol 162:107–130.

Gao K-Q, Shubin NH. 2001. Late Jurassic salamanders from northern China. Nature 410:574–577.

Gillis GB. 1997. Anguilliform locomotion in an elongate salamander (*Siren intermedia*): effects of speed on axial undulatory movements. J Exp Biol 200:767–784.

Gillis GB, Blob RW. 2001. How muscles accommodate movement in different physical environments: aquatic vs. terrestrial locomotion in vertebrates. Comp Biochem Physiol A 131:61–75.

Gray J. 1968. Animal locomotion. New York: WW Norton & Company.

He J, Kram R, McMahon TA. 1991. Mechanics of running under simulated low gravity. J Appl Physiol 71:863–870.

Hildebrand M. 1966. Analysis of the symmetrical gaits of tetrapods. Fol Biotheor 6:9–22.

Hildebrand M. 1976. Analysis of tetrapod gaits: general considerations and symmetrical gaits. In: Herman RM, Grillner S, Stein PSG, Stuart DG, editors. Neural control of locomotion. New York: Plenum Press. p 203–236.

Hildebrand M. 1985. Walking and running. In: Hildebrand M, Bramble D, Liem KF, Wake D, editors. Functional vertebrate morphology. Cambridge, MA: Belknap Press of Harvard University Press. p 38–57.

Ijspeert AJ. 2000. A 3-D biomechanical model of the salamander. In: Heudin J-C, editor. Proceedings of the second international conference on virtual worlds. Heidelberg, Germany: Springer. p 225–234.

Ijspeert AJ. 2001. A connectionist central pattern generator for the aquatic and terrestrial gaits of a simulated salamander. Biol Cybern 84:331–348.

Ijspeert AJ, Crespi A, Ryczko D, Cabelguen J-M. 2007. From swimming to walking with a salamander robot driven by a spinal cord model. Science 315:1416–1420.

Irschick DJ, Jayne BC. 1999. Comparative three-dimensional kinematics of the hindlimb for high-speed bipedal and quadrupedal locomotion of lizards. J Exp Biol 202:1047–1065.

Johansson LC, Lindhe-Norberg UM. 2001. Lift-based paddling in diving grebe. J Exp Biol 204:1687–1696.

Liao JC. 2004. Neuromuscular control of trout swimming in a vortex street: implications for energy economy during the Karman gait. J Exp Biol 207:3495–3506.

Lindhe-Norberg UM, Brooke AP, Trewhella WJ. 2000. Soaring and non-soaring bats of the family pteropodidae (flying foxes, *Pteropus* spp.): wing morphology and flight performance. J Exp Biol 203:651–664.

Martinez MM. 1996. Issues for aquatic pedestrian locomotion. Am Zool 36:619–627.

Martinez MM. 2001. Running in the surf: hydrodynamics of the shore crab *Grapsus tenuicrustatus*. J Exp Biol 204: 3097–3112.

Martinez MM, Full RJ, Koehl MAR. 1998. Underwater punting by an intertidal crab: a novel gait revealed by the kinematics of pedestrian locomotion in air versus water. J Exp Biol 201:2609–2623.

Müller UK, van Leeuwen JL. 2004. Swimming of larval zebrafish: ontogeny of body waves and implications for locomotory development. J Exp Biol 207:853–868.

Nauwelaerts S, Ramsay J, Aerts P. 2007. Morphological correlates of aquatic and terrestrial locomotion in a semi-aquatic frog, *Rana esculenta*: no evidence for a design conflict. J Anat 210:304–317.

Peters SE, Goslow GE. 1983. From salamanders to mammals: continuity in musculoskeletal function during locomotion. Brain Behav Evol 22:191–197.

Petranka JW. 1998. Salamanders of the United States and Canada. Washington, DC: Smithsonian Institution Press.

Pridmore PA. 1992. Trunk movements during locomotion in the marsupial *Monodelphis domestica* (Didelphidae). J Morphol 211:137–146.

Pridmore PA. 1994. Submerged walking in the epaulette shark *Hemiscyllium ocellatum* (Hemiscyllidae) and its implications for locomotion in rhipidistian fishes and early tetrapods. Zool Anal Complex Syst 98:278–297.

Reilly SM, Elias JA. 1998. Locomotion in *Alligator mississippiensis*: kinematic effects of speed and posture and their relevance to the sprawling-to-erect paradigm. J Exp Biol 201:2559–2574.

Renous S, Hofling E, Gasc JP. 1999. On the rhythmical coupling of the axial and appendicular systems in small terrestrial lizards (Sauria: Gymnophthalmidae). Zool Anal Complex Syst 102:31–49.

Rewcastle SC. 1981. Stance and gait in tetrapods: an evolutionary scenario. Symp Zool Soc Lond 48:239–267.

Rice WR. 1989. Analyzing tables of statistical tests. Evolution 43:223–225.

Ritter D. 1992. Lateral bending during lizard locomotion. J Exp Biol 173:1–10.

Rosenhahn B, Brox T, Cremers D, Seidel H-P. 2007. Online smoothing for markerless motion capture. In: Hamprecht FA, Schnörr C, Jähne B, editors. Pattern recognition: twenty-nineth DAGM symposium. Heidelberg, Germany: Springer. p 163–172.

Snyder RC. 1949. Bipedal locomotion of the lizard *Basiliscus basiliscus*. Copeia 1949:129–137.

Swartz SM, Bennett MB, Carrier DR. 1992. Wing bone stresses in free flying bats and the evolution of skeletal design for flight. Nature 359:726–729.

Swayne DF, Lang DT, Buja A, Cook D. 2003. GGobi: Evolving from XGobi into an extensible framework for interactive data visualization. Comput Stat Data Anal 43:423–444.

Taylor T, Massey C. 2001. Recent developments in the evolution of morphologies and controllers for physically simulated creatures. Artif Life 7:77–87.

Thorsen DH, Cassidy JJ, Hale ME. 2004. Swimming of larval zebrafish: fin–axis coordination and implications for function and neural control. J Exp Biol 207:4175–4183.

Vint P, Hinrichs R. 1996. Endpoint error in smoothing and differentiating raw kinematic data: an evaluation of four popular methods. J Biomech 29:1637–1642.

Vogel S. 1994. Life in moving fluids. Princeton: Princeton University Press.

Vogel S. 2003. Comparative biomechanics. Princeton: Princeton University Press.

Wheatley M, Edamura M, Stein RB. 1992. A comparison of intact and in-vitro locomotion in an adult amphibian. Exp Brain Res 88:609–614.